Enhanced heat transfer through filler-polymer interface by surface-coupling agent in heat-dissipation material: A non-equilibrium molecular dynamics study

Kouichi Tanaka, Shuji Ogata, Ryo Kobayashi, Tomoyuki Tamura, Masashi Kitsunezuka, and Atsushi Shinma

Citation: Journal of Applied Physics **114**, 193512 (2013); doi: 10.1063/1.4831946
View online: http://dx.doi.org/10.1063/1.4831946
View Table of Contents: http://scitation.aip.org/content/aip/journal/jap/114/19?ver=pdfcov
Published by the AIP Publishing

Enhanced heat transfer through filler-polymer interface by surface-coupling agent in heat-dissipation material: A non-equilibrium molecular dynamics study

Kouichi Tanaka,[1,2] Shuji Ogata,[2] Ryo Kobayashi,[2] Tomoyuki Tamura,[2]
Masashi Kitsunezuka,[1] and Atsushi Shinma[1]
[1]*DENSO CORPORATION, Kariya, Aichi 448-8661, Japan*
[2]*Graduate School of Engineering, Nagoya Institute of Technology, Nagoya 466-8555, Japan*

(Received 17 July 2013; accepted 3 November 2013; published online 19 November 2013)

Developing a composite material of polymers and micrometer-sized fillers with higher heat conductance is crucial to realize modular packaging of electronic components at higher densities. Enhancement mechanisms of the heat conductance of the polymer-filler interfaces by adding the surface-coupling agent in such a polymer composite material are investigated through the non-equilibrium molecular dynamics (MD) simulation. A simulation system is composed of α-alumina as the filler, bisphenol-A epoxy molecules as the polymers, and model molecules for the surface-coupling agent. The inter-atomic potential between the α-alumina and surface-coupling molecule, which is essential in the present MD simulation, is constructed to reproduce the calculated energies with the electronic density-functional theory. Through the non-equilibrium MD simulation runs, we find that the thermal resistance at the interface decreases significantly by increasing either number or lengths of the surface-coupling molecules and that the effective thermal conductivity of the system approaches to the theoretical value corresponding to zero thermal-resistance at the interface. Detailed analyses about the atomic configurations and local temperatures around the interface are performed to identify heat-transfer routes through the interface. © *2013 AIP Publishing LLC*. [http://dx.doi.org/10.1063/1.4831946]

I. INTRODUCTION

The integrated circuit (IC)-utilized modular packaging of electronic components for automobiles has advanced remarkably in recent years.[1,2] It is beneficial to automobiles not only for their compactness but also for reliability and functionality. Such modular packaging has been essential particularly for the electric and plug-in hybrid automobiles. Further improvement of the packaging toward higher densities is therefore desired. One of the important techniques that should be realized in developing the higher-density packaging is efficient dissipation of intense heat generated locally, e.g., in a power IC.[1–3] Heat-dissipation material for that purpose in the forms of adhesive and bulking agent needs be soft to cover an IC without gaps. Composite systems of soft polymers and hard filler-particles (called fillers) are often used for such heat-dissipation materials.[2,4,5] The fillers, which are about $1-10$ μm in size, are made of the materials with higher thermal conductivities than the polymers for enhanced effective thermal conductivity of the heat-dissipation material. For its application to IC's, the heat-dissipation material should be electrically insulating.[6] Automobile-parts companies have been putting great effort to design a novel heat-dissipation material with a few times higher thermal conductivity than the current ones under the conditions that it is electrically insulating, durable, and low cost.

Many papers have been published to propose or demonstrate various techniques for higher thermal conductivities of such polymer composite materials.[7–10] The techniques include: charging of fillers, usage of fillers with higher thermal conductivities, and controlled agglomeration of fillers. With the techniques, however, enhancement factors of the thermal conductivities of polymer composite materials are still behind expectation due to high thermal resistances at the filler-polymer interfaces. Reducing the thermal resistance at the interface is the key.

The interface in the polymer composite material is characterized as the co-existence system of hard inorganic and soft organic materials. Phonons that transfer heat are scattered by the interface due to difference in hardness and mass density, leading to substantial thermal resistance.[11] To reduce the thermal resistance at the interface, surfaces of fillers are often coated by the surface-coupling (SC) agent. The surface-coupling agent, which is made of organic molecules, acts to connect fillers and polymers tightly. It has been experimentally demonstrated that adding the silane coupling agent enhances the effective thermal conductivity of the polymer composite material.[9,10]

Detailed experimental analyses of the enhancement mechanisms have not been performed because the interfaces are intrinsically nanometer-sizes. It is therefore difficult to predict the maximum enhancement factor of the effective thermal conductivity that we can reach by modifying the surface-coupling agent.

Theoretical approach with the classical molecular dynamics (MD) simulation has potential capability to address the issue of understanding the enhancement mechanisms of the thermal conductivity of the polymer composite material by the surface-coupling molecules. There exist various classical MD simulation studies about the evaluation of thermal conductivities of bulk materials.[12–16] On the other hand, a

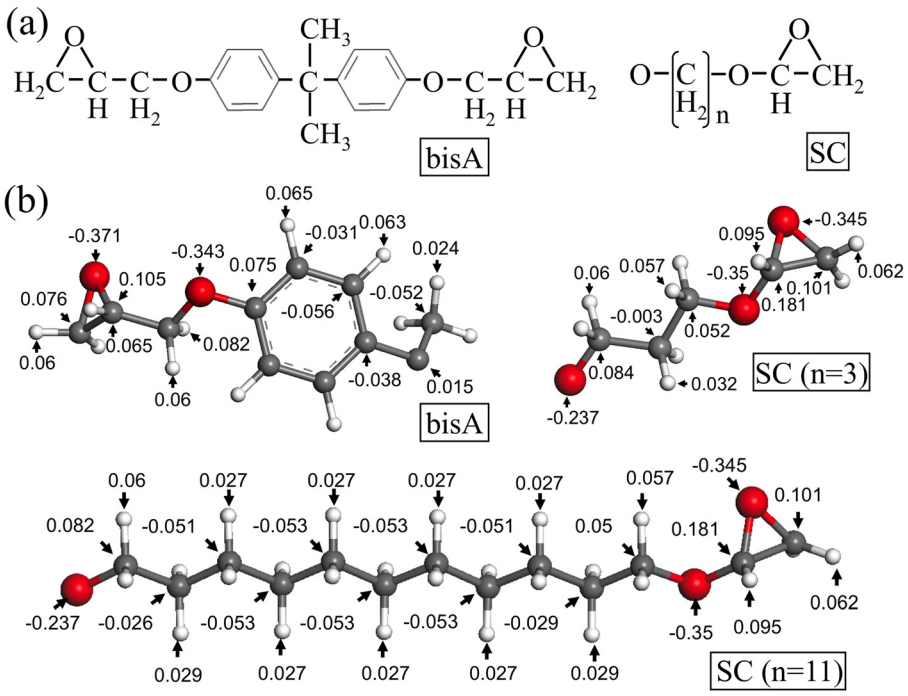

FIG. 1. (a) Structure of bisphenol-A (bisA) and model SC molecules. (b) Atomic charges in unit of e of the bisA molecule (equivalent atoms are omitted for symmetry) and SC molecules with $n = 3$ and 11.

limited number of papers, to investigate the interface of dissimilar materials.[17–21] Luo and Lloyd[21] reported their interesting work about the effective thermal conductivity of the interface between polymers and either graphene or graphite. Complication exists in preparation of a reliable set of inter-atomic potentials between filler, polymer, and surface-coupling molecule for the MD simulation of the polymer composite material.

In the present paper, we will first construct a set of inter-atomic potentials for a model polymer composite material with surface-coupling molecules. We will add an original inter-atomic potential that is based on the electronic density-functional theory (DFT) to two suites of inter-atomic potentials for polymers and fillers, respectively. We will then perform the non-equilibrium MD simulation to obtain the temperature profile and heat flux in the system. Effects of the surface-coupling molecules on heat transfer will be analyzed by changing their lengths and density. We will investigate the atomistic details of the heat-transfer routes in the system.

The remaining sections are organized as follows. In Sec. II, atomistic modeling of the simulation system and preparation of the inter-atomic potentials will be explained. Section III will analyze size-effect on the thermal conductivity calculated with the non-equilibrium MD simulation to set a proper size and temperature of the system for the present simulation. Section IV will perform the non-equilibrium MD runs at various settings of the surface-coupling molecules to understand their effects on the heat transfer. Summary and concluding remarks will be given in Sec. V.

II. MODELING OF SYSTEM AND PREPARATION OF INTER-ATOMIC POTENTIALS

In the present simulation study, we assume α-alumina for the filler and bisphenol-A (bisA) epoxy for the polymer (see, Fig. 1(a)) because both are commonly used for the electrically insulating heat-dissipation composite material. For the surface-coupling agent, the silane composite molecule is often used. The silane composite molecule is basically composed of two kinds of groups attached to a Si atom: the reaction group (e.g., epoxy) bonds to an organic polymer, while the OR group (e.g., $-O-CH_3$) undergoes the hydrolysis reaction to form a strong bond between the O and a surface atom of an inorganic filler.[10] The silane composite molecule thereby works to bind a filler and polymer together. In the present simulation, we use a virtual SC molecule shown in Fig. 1(a) that mimics the state after the hydrolysis reaction: an epoxy group connects to $(CH_2)_n$ while the other end of $(CH_2)_n$ is saturated with an O atom. We set n of $(CH_2)_n$ to either 3 or 11.

We use the following form of two-body inter-atomic interaction potentials for Al and O in α-alumina in a potential suite developed for the MD simulation of CaO, MgO, Al_2O_3, and SiO_2 systems and coined CMAS potential:[22]

$$V(r_{ij}) = \frac{q_i q_j}{r_{ij}} - \sqrt{\epsilon_i \epsilon_j}\left(\frac{\sigma_i + \sigma_j}{2r_{ij}}\right)^6 + (B_i + B_j) f \exp\left(\frac{A_i + A_j - r_{ij}}{B_i + B_j}\right), \quad (1)$$

with the atomic charges $\{q_i\}$ and parameters $\{A_i\}$, $\{B_i\}$, $\{\epsilon_i\}$, $\{\sigma_i\}$, and f. The Dreiding inter-atomic potentials[23] are applied to the bisA and SC molecules:

$$V = \sum_{(i,j)} \frac{K_{ij}}{2}(r_{ij} - r_{ij,\mathrm{eq}})^2 + \sum_{(i,j,k)} K_{ijk}(\theta_{ijk} - \theta_{ijk,\mathrm{eq}})^2 + \sum_{(i,j,k,l)} \frac{V_{jk}}{2}\{1 - \cos[n_{jk}(\varphi_{ijkl} - \varphi_{ijkl,\mathrm{eq}})]\} + \sum_{(i,j)} \sqrt{\epsilon_i \epsilon_j}\left[\left(\frac{\sigma_i + \sigma_j}{2r_{ij}}\right)^{12} - \left(\frac{\sigma_i + \sigma_j}{2r_{ij}}\right)^6\right] + \sum_{(i,j)} \frac{q_i q_j}{r_{ij}}, \quad (2)$$

with the atomic charges $\{q_i\}$ and various parameters $\{K_{ij}\}$, $\{K_{ijk}\}$, $\{V_{jk}\}$, $\{r_{ij,\mathrm{eq}}\}$, $\{\theta_{ijk,\mathrm{eq}}\}$, $\{n_{jk}\}$, $\{\varphi_{ijkl,\mathrm{eq}}\}$, $\{\epsilon_i\}$, and $\{\sigma_i\}$. In Eq. (2), the bonded inter-atomic interaction is described by the two-body bonding, three-body angle, and four-body torsion terms, while the non-bonded one by the van der Waals and Coulomb terms; the non-bonded interaction with up to the third nearest neighbor atoms is omitted. We need to determine the atomic charges $\{q_i\}$ in Eq. (2) for the bisA and SC molecules. Following the Gasteiger-Marsili method,[24] we obtain the charges as solutions to a set of generalized electronegativity equalization equations for the corresponding sigma-bond model system for each kind of molecules. The calculated values of the charges are typed in Fig. 1(b).

We need to construct the inter-atomic potential between the SC molecule and α-alumina. To calculate the energies at various configurations of them, we use the DMol^3 software package[25,26] in Materials Studio 5.5 with the PBE[27] form of the generalized gradient approximation for the exchange-correlation potential. The energy tolerance in the self-consistency field iteration is set to 5×10^{-5} eV per atom. As for the basis set for the electron orbitals, we use the double numerical with polarization (DNP) set recommended in the DMol^3 for high accuracy purposes. As an accuracy check, we calculate the cohesion energy of bulk α-alumina to find 2.6 eV per Al-O bond and the elastic constants $C_{11} = 518$ GPa and $C_{33} = 494$ GPa. Their differences from the experimental values are as small as 5%.[28,29]

We consider (0001) surface of α-alumina as the filler surface, which is the most stable one when terminated with Al.[30–32] As depicted in Fig. 2, a thin α-alumina slab of 120 atoms with (0001) surface is placed in the rectangular parallelepiped of $(L_x, L_y, L_z) = (14.0\ \text{Å}, 8.2\ \text{Å}, 7.0\ \text{Å})$; the vacuum layer with z-depth 20 Å is added on the (0001) surface. The periodic boundary conditions are applied in the three directions. Using the DMol^3 package, geometry optimization is performed for the system. The outermost Al atoms sink to lie nearly on the same O-plane as reported in a former paper.[30] We then place a single SC molecule on the (0001) surface to find the most stable configuration. Figure 2(a) depicts the most stable configuration obtained through the relaxation runs starting with various settings of the SC molecule including the case with 45° inclined toward the (0001) surface. We find that the O atom at the end of the SC molecule bonds tightly to a surface Al atom.

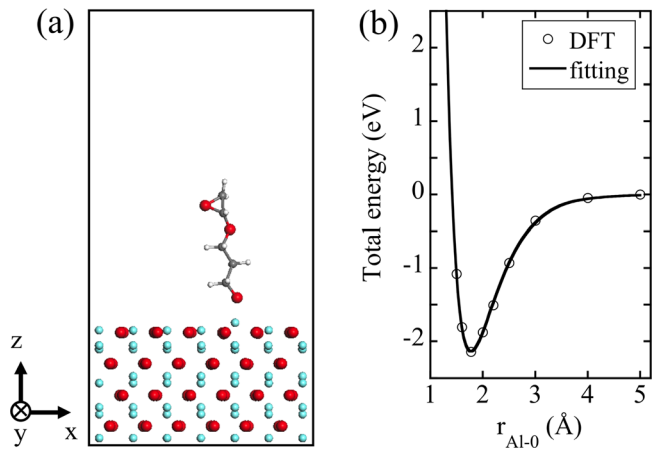

FIG. 2. (a) Ground-state configuration of a SC molecule on (0001) surface of α-alumina. Large red spheres are O; small cyan, Al; medium grey, C; small white, H. (b) Total energy of the system in (a) as a function of $r_{\mathrm{Al-O}}$.

The binding energy, which is defined as the difference in the total energy between the well-separated and ground-state configurations, is 2.06 eV; the Al-O distance $r_{\mathrm{Al-O}} = 1.77$ Å. The binding energy is smaller by 20% than the cohesive energy per Al-O bond of bulk α-alumina; the $r_{\mathrm{Al-O}}$ is shorter by $0.1 - 0.2$ Å than the average in bulk α-alumina. Figure 2(b) shows the total energy minus the value at $r_{\mathrm{Al-O}} = 5.0$ Å as a function of $r_{\mathrm{Al-O}}$; for each value of $r_{\mathrm{Al-O}}$, all the other atoms are relaxed. We fit the calculated energies to the Morse potential form

$$V(r_{\mathrm{Al-O}}) = D\{1 - \exp[-\beta(r_{\mathrm{Al-O}} - r_0)]\}^2 - D, \quad (3)$$

with $D = 2.06$ eV, $r_0 = 1.77$ Å, and $\beta = 1.93$ Å^{-1}.

For the inter-atomic interaction between α-alumina and SC molecules and between α-alumina and bisA molecules, we first adopt the van der Waals and Coulomb terms in Eqs. (1) and (2) with the same parameter values for pure α-alumina, SC, and bisA systems. For each bonding pair of Al atom of α-alumina and O atom of the SC molecule, we then subtract the van der Waals and Coulomb terms and apply Eq. (3).

III. PREPARATORY SIMULATION

We determine the proper size of the simulation system from following analyses. It has been remarked that the thermal conductivity of a bulk material calculated using the non-equilibrium MD simulation method often shows a significant system-size dependence.[14–16] In the method, two well-separated slab areas in the system are controlled to different temperatures. The input and output fluxes of heat at the temperature-controlled areas are calculated in the steady state. Using the temperature gradient at a proper position, the heat flux, and the distance between the areas, we calculate the thermal conductivity (see, Eq. (4) below). If the system size is shorter than the mean free-path of phonons, the thermal conductivity is underestimated because the phonons are scattered artificially at the temperature-controlled areas.[14–16] In the present simulation of the interface system containing α-alumina and bisA regions, changing the width of the α-alumina region gives no significant effect on the overall thermal resistance of the system because the thermal resistance of bisA is much higher than that of α-alumina. In the following, we determine the width of the bisA region heuristically by performing separately various non-equilibrium MD runs for pure bisA systems.

We prepare the bisA systems with $(L_x, L_y, L_z) = (34\ \text{Å}, 38\ \text{Å}, 62\ \text{Å})$, $(34\ \text{Å}, 38\ \text{Å}, 112\ \text{Å})$, and $(34\ \text{Å}, 38\ \text{Å}, 224\ \text{Å})$ under the periodic boundary conditions to perform the non-equilibrium MD simulation runs. In the three systems, the bisA molecules form amorphous solids with the same mass density of 0.90 g/cm^3. The average temperatures of the system are $T = 300$ K, 400 K, and 500 K. The two ends of the system are controlled to $T + 20$ K,

while the central area to $T-20$ K. Since the bisA molecules diffuse slightly at those temperatures, the number of atoms located in each temperature-control area with 6.2 Å z-width fluctuates in time (for instance, 600–700 in the low-temperature control area in the run at $T=500$ K) but shows no tendency of drift after 0.1 ns. We use the temperature profile at a z-range that is well separated (>10 Å) from the temperature-control areas to obtain a reliable value for the thermal conductivity. At $T=300$ K, the thermal conductivities are calculated as 0.07, 0.08, and 0.12 $\mathrm{W/m\cdot K}$ for the cases with $L_z=62$ Å, 112 Å, and 224 Å, respectively. The present value, 0.12 $\mathrm{W/m\cdot K}$, of the thermal conductivity for the case of $L_z=224$ Å is close to the experimental values in the range of $0.15-0.25$ $\mathrm{W/m\cdot K}$ at room temperatures.[7] At $T=400$ K and 500 K, the thermal conductivity appears to be saturated to $0.11-0.13$ $\mathrm{W/m\cdot K}$ for $L_z\geq 112$ Å. It is confirmed that increasing the temperature difference between the two ends to 60 K gives the same value within error bars for the thermal conductivity. Considering those, we set the z-width of the bisA region to 112 Å and the system temperature to $T=400$ K with plus 30 and minus 30 K at the temperature-control areas in the present simulation runs.

A typical configuration of the system in the present non-equilibrium MD simulation is depicted in Fig. 3. It corresponds to the case with no SC molecule. The periodic boundary conditions are applied in the three directions. The system is a rectangular parallelepiped with dimensions $(L_x,\ L_y,\ L_z)=(34$ Å, 38 Å, 168 Å$)$; it is composed of 18 656 atoms. The left and right 6.2 Å z-width ends are controlled to $T=430$ K, while the central 12.4 Å z-width to $T=370$ K. The simulation system contains the bisA region with 112 Å in z-width at the center, which is sandwiched in z-direction between the α-alumina regions. Note that the α-alumina regions are connected to each other from the periodicity of the system. In a simulation run, the velocity-Verlet algorithm is used to integrate the equations of motion. The temperature is controlled with the simple velocity-scaling method. We set the time step $dt=1.0$ fs from detailed analyses about the dt-dependencies of the temperature profile and energy flux for a practical system, which will be explained in Sec. IV A.

By controlling the temperatures of the center (bisA) and two ends (α-alumina) of the system to low and high values, respectively, as shown in Fig. 3, we produce heat fluxes that direct from the α-alumina to bisA regions. We calculate the effective thermal conductivity λ of the system after the steady state is realized as

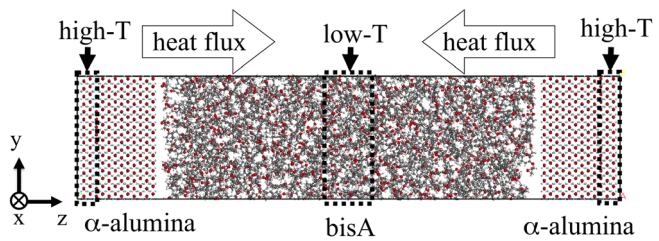

FIG. 3. Atomic configuration of the system with no SC molecule in the present simulation.

$$\lambda=\frac{Jl}{T_1-T_2}\ , \tag{4}$$

where J is the heat flux per unit time and surface area, T_1 and T_2 are the high and low temperatures of well-separated z-positions under the condition that both are not close to the temperature-control areas, and l is the distance between the high- and low-temperature positions. In a simulation run, we confirm that the system is in the steady state by comparing the input and output energies per unit time in the temperature-controlled bins. The J and temperature profile are obtained as averages over 0.5 ns in the steady state.

IV. NON-EQUILIBRIUM MD SIMULATION RESULTS

A. Temperature profile and thermal conductivity

We here add the SC molecules to the system to analyze their effects on heat transfer through the interface. For the analyses, we need to compare the results for various settings of the SC molecules. For $n=3$ of $(CH_2)_n$ of the SC molecule, number of the SC molecules in the system is {1, 4, 8, 16, 32}. For $n=11$, the number of the SC molecules is 16. We arrange the SC molecules that bond to surface Al atoms in a square-lattice form as depicted in Fig. 4; such Al-O bonds are kept during a run. At the addition of the SC molecules, we need to increase L_z of the system from the original value of $L_z=168$ Å (no SC molecule) so that the averaged mass density does not change from 1.85 $\mathrm{g/cm^3}$.

We set the time step, dt, to a proper value by comparing simulation results for a typical system between with $dt=0.5$ and 1.0 fs. For the purpose, the case of containing a 16 SC molecules with $n=3$, denoted as M16n3, is considered. Figure 5(a) depicts the energy fluxes, J, in the two runs; the positive values correspond to the input fluxes to the high-temperature control area, while the negative values to the output fluxes from the low-temperature control area. Even with $dt=1.0$ fs, the input and output fluxes agree well with each other indicating no system heat-up. Figure 5(b) shows the temperature profile of the bisA region in the system. We here consider the bisA region only because the temperature profile is flat in the α-alumina region (see, Fig. 6). The

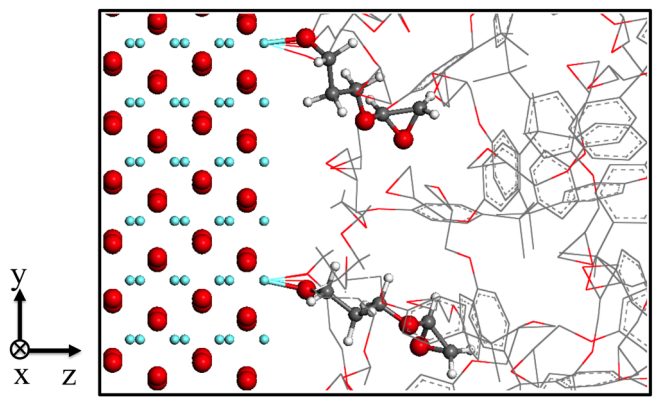

FIG. 4. (a) Atomic configuration of SC molecules on (0001) surface of α-alumina in the M16n3 case viewed from x-direction. Large red spheres are O; small cyan, Al; medium grey, C; small white, H. The bisA molecules are drawn by sticks.

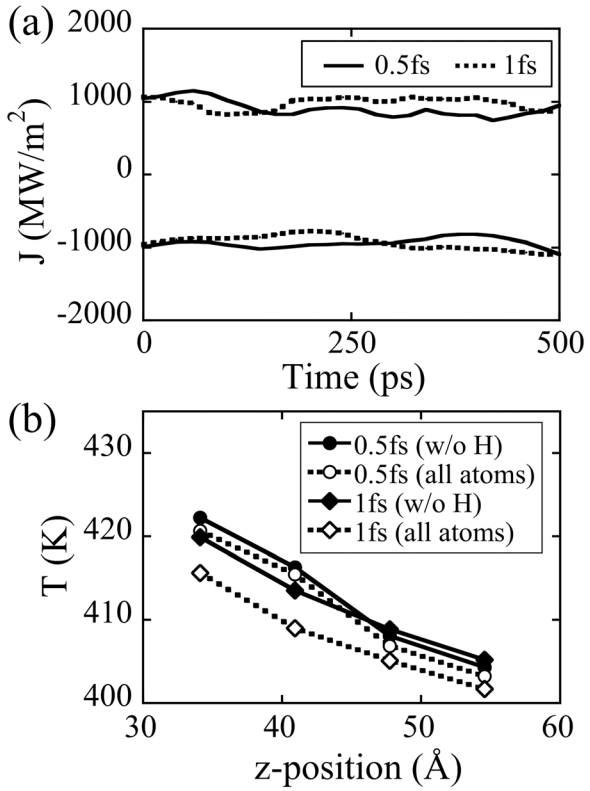

FIG. 5. (a) Time evolution of J in the high- and low-temperature control areas for the M1n3 case. The solid curve corresponds to the time step 0.5 fs; dotted curve, to 1.0 fs. (b) Temperature profiles in the bisA with SC region in the M1n3 case. The profiles are calculated either for all atoms (open symbols) or without H (filled symbols).

temperature profile in Fig. 5(b) is obtained as the average of two profiles with the z measuring from the center to the left and right of the system, respectively (see, Fig. 3). The α-alumina region correspond to $z = 0$–26 Å. The low-temperature control area corresponds to $z = 70$–85 Å. We find in Fig. 5(b) that the temperatures calculated for all atoms in the 1.0 fs run deviate substantially from the reference ones in the 0.5 fs run. Interestingly, however, the temperatures

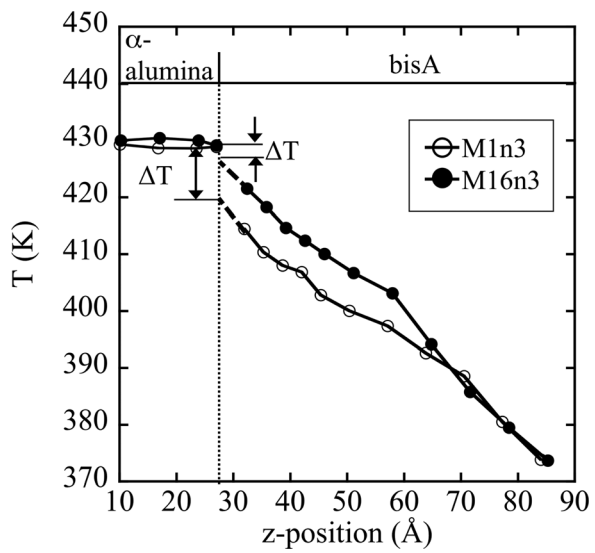

FIG. 6. Temperature profiles in the M1n3 and M16n3 cases.

calculated without H atoms in the 1.0 fs run agree well with the reference ones as seen in Fig. 5(b). Since the calculated temperatures change little (<1.3 K), if we omit H atoms in the 0.5 fs run, we consider that such a substantial temperature change seen in the 1.0 fs run is related to the fast vibration of H. From those observations about the J and temperature profile, we choose to set $dt = 1.0$ fs for fast simulation and omit H atoms to calculate the temperature profile.

Figure 6 shows the detailed temperature profiles in two typical cases: one is the M16n3 case and the other is the case of a single SC molecule with $n = 3$ denoted as M1n3. The dashed line in Fig. 6 represents the extrapolation of the two data points near the interface in the bisA region. Since the end z-position of the bisA with SC region fluctuates in time and varies depending on the x-y location, we set it as the one separated by 2.0 Å from the end (i.e., Al) of α-alumina, therefore, at $z = 28$ Å. We use $z = 28$ Å to predict the local temperature of the bisA with SC region at the interface. The temperature profiles are almost flat in the α-alumina region, while linearly decreasing profiles are seen in the bisA region in both cases. Such difference originates from the large difference in the thermal conductivity between α-alumina and bisA. Particularly in the M1n3 case, the temperature-gap ΔT at the interface is substantial. In both cases, there exist obvious changes at $z = 60$–70 Å in the temperature lowering behavior as z is increased. We consider that the changes are reflections of the artificial temperature control in the bisA region at $z = 70$–85 Å. The temperature profile is therefore physically reliable in the range $z = 10$–50 Å only.

To calculate the thermal conductivity, $\lambda = Jl/(T_1 - T_2)$ in Eq. (4), of the system, we choose a z-position of high temperature (T_1) at $z = 0$ Å in the α-alumina region and that of low temperature (T_2) at $z = 80$ Å in the bisA region; that is, $l = 80$ Å. Since the temperature profiles in Fig. 6 are reliable only in the range of $z = 10 - 50$ Å, we evaluate T_1 and T_2 as follows. Due to the flatness of temperatures in the α-alumina region seen in Fig. 6, we can assume $T_1 = 430$ K. As for T_2, we first obtain the least-squared fitted line of the data points in the range $z = 35 - 50$ Å and secondary extrapolate the line to $z = 80$ Å. Table I compares thereby calculated values of J, ΔT, $J/\Delta T$, and λ in all the cases. The J is obtained as the average of input and output fluxes of heat; the relative difference between the two is less than 5% in all the cases.

The λ and $J/\Delta T$ in Table I enlarge by increasing either lengths (n) or number of the SC molecules, which suggests that a substantial proportion of heat flows through the SC molecules. We note that ΔT is quite sensitive to the setting of the SC molecules, while the flux J is insensitive to that. In the M32n3 case, ΔT is as small as 1.9 K. It is because thermal resistance of the interface is small due to large number (32) of the SC molecules. In fact, $J/\Delta T$ in the M32n3 case is 6.8 times as high as that in the M1n3 case. However, as the contribution of the bisA region to the effective thermal resistance is dominant, λ in the M32n3 case is only 1.4 times as large as that in the M1n3 case. Figure 7 shows such a relations between λ and $J/\Delta T$. The λ appears to be saturated for large $J/\Delta T$, the estimated saturation-limit value of

TABLE I. The J, ΔT, $J/\Delta T$, and λ obtained in various cases of the present simulation.

Case	Number of SC molecules	n of $(CH_2)_n$	J (W/m^2)	ΔT (K)	$J/\Delta T$ $(W/m^2 \cdot K)$	λ $(W/m \cdot K)$
M0	0	…	8.17×10^8	9.6	8.51×10^7	0.119
M1n3	1	3	8.10×10^8	10.8	7.50×10^7	0.127
M4n3	4	3	8.68×10^8	8.1	1.07×10^8	0.131
M8n3	8	3	9.12×10^8	7.4	1.23×10^8	0.136
M16n3	16	3	9.25×10^8	4.3	2.15×10^8	0.157
M16n11	16	11	1.02×10^9	3.5	2.92×10^8	0.158
M32n3	32	3	9.63×10^8	1.9	5.07×10^8	0.181

0.185 $W/m \cdot K$ compares well with the theoretical value calculated using the present thermal conductivity 0.12 $W/m \cdot K$ of bulk bisA multiplied by the inverse of the z-width proportion $(52/80 = 0.65)$ of the bisA region in the system.

B. Heat-transfer routes through interface

We investigate heat transfer routes from the α-alumina (i.e., filler) to bisA molecules (i.e., polymers) when the SC molecules are added in between. As stated above, a substantial proportion of heat flows from the α-alumina to SC molecules. It is because the SC molecules bond tightly to the α-alumina surface. We therefore consider the heat-transfer routes from the SC to bisA molecules by calculating the atomic temperature, defined as the time-averaged kinetic energy of a single atom in energy unit, for each atom around the SC molecules. We assume[21] that the difference in the atomic temperatures of a pair of atoms gets larger as the degree of thermal resistance between the two atoms becomes larger. With the assumption, we compare the atomic temperatures of all atoms of the SC and neighboring bisA molecules to find the heat-transfer routes.

Figure 8(a) shows the atomic temperatures of the SC molecule and surface Al in the M8n3, M16n3, and M32n3 cases. The sequence in the horizontal axis corresponds to that in the SC molecule. The atomic temperatures in the M16n11 case (i.e., longer SC molecule) are shown in Fig. 8(b). Averages over the equivalent atoms of the SC molecules are performed in Fig. 8. As the error bars in Fig. 8 indicate, the atomic temperatures have accuracies of 0.5 – 1.5 K. We remind that the atomic temperatures agree among atoms (excluding H atoms) within 0.5 – 1.5 K in an equilibrium run of a bulk bisA system at $T = 400$ K.

We find in Fig. 8(a) that the atomic temperatures of the SC molecules in the M16n3 and M32n3 cases are much closer to that of the surface Al as compared to the M8n3 case. In the M16n3 and M32n3 cases, heat is therefore transferred more efficiently between the α-alumina and SC molecule and inside the SC molecule than between the SC and bisA molecules. Similar relatively efficient heat transfer

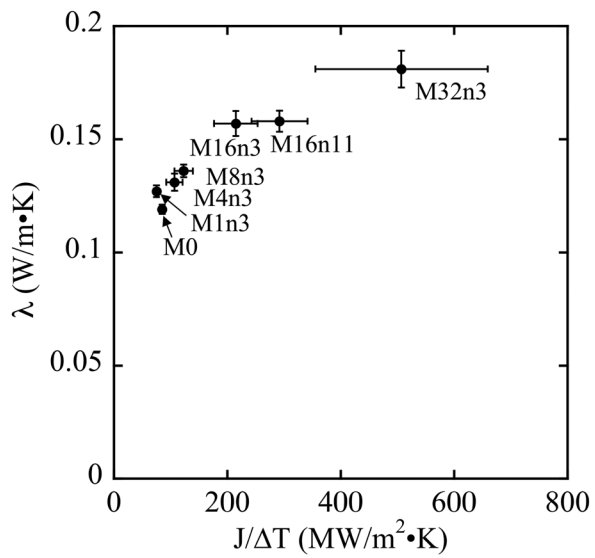

FIG. 7. Relation between λ and $J/\Delta T$ in the present runs. Possible errors estimated are also drawn.

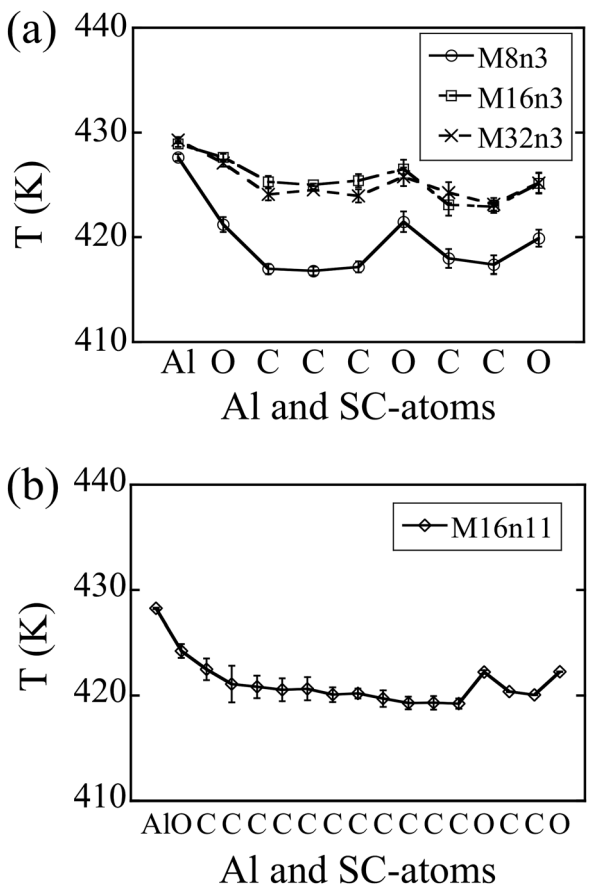

FIG. 8. (a) Atomic temperatures of both surface Al atoms that bond to SC molecules and SC atoms in the M8n3, M16n3, and M32n3 cases. Possible errors estimated are also drawn. (b) Same as (a) but in the M16n11 case.

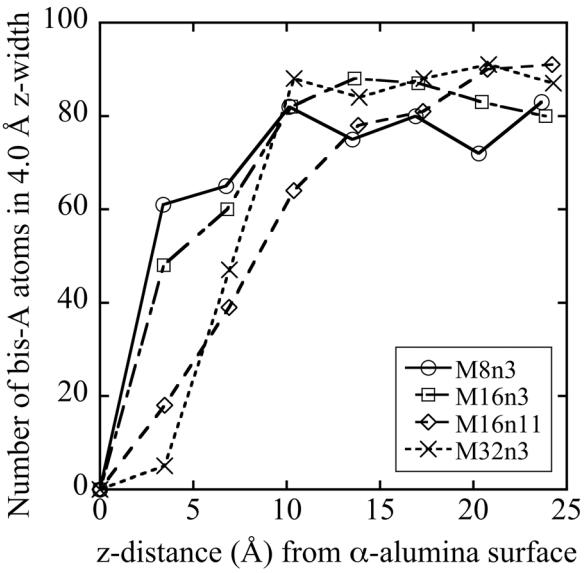

FIG. 9. Numbers of bisA atoms in the 4.0 Å z-width bins prepared virtually from the α-alumina surface in the M8n3, M16n3, M16n11, and M32n3 cases.

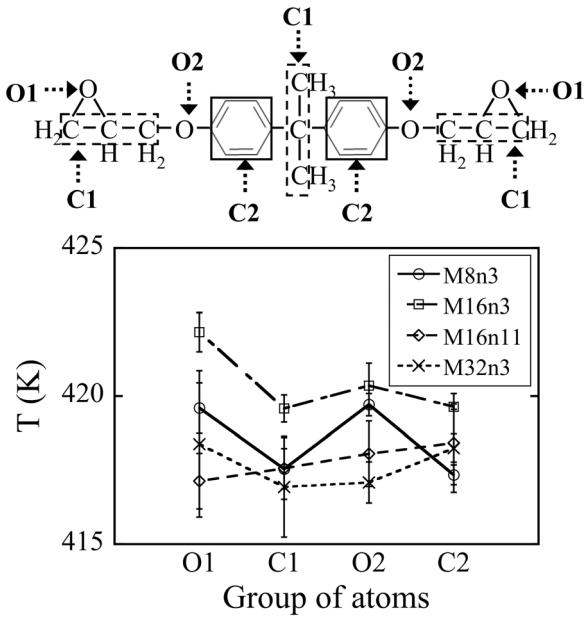

FIG. 10. (top) Grouping of bisA atoms. (bottom) Atomic temperatures of the groups in M8n3, M16n3, M16n11, and M32n3 cases. Possible errors estimated are also drawn.

inside the SC molecule is observed in the M16n11 case in Fig. 8(b). In the M8n3 case, on the other hand, heat transfer is more efficient between the SC and bisA molecules than between the α-alumina and SC molecule and inside the SC molecule. Since the bonding state of the Al-O pair between the α-alumina and SC molecule and therefore its heat resistivity are essentially unchanged in all the cases, we conclude that heat flux from the SC to bisA molecules is impeded more in the M16n3, M32n3, and M16n11 cases than in the M8n3 case. Due to the large number of the SC molecule in the M32n3 case, however, such relatively high thermal impedance from the SC to bisA molecules contributes little to the overall thermal resistance.

We explain physical reasons of the relatively high thermal impedance between the SC and bisA molecules for both cases of large number (32) and long lengths ($n = 11$) of SC molecules. Figure 9 shows the numbers of bisA atoms in the 4.0 Å z-width bins prepared virtually from the α-alumina surface. The number approaches to the bulk value of around 85 in all the cases for $z > 15$ Å. By increasing either number of the SC molecules to 32 or length (n) of the SC molecule to 11, we find that the bisA atoms are pushed away significantly from the α-alumina surface. Since effective interaction between the SC and bisA molecules becomes weaker in the situation, heat transfer from the SC to bisA molecules is impeded. On the contrary, there exist substantial number of bisA atoms near the α-alumina surface in the M8n3 case. Those bisA atoms entangle the SC molecules, resulting in relatively efficient heat-transfer from the SC to bisA molecules.

We now consider the heat-transfer routes from the SC to bisA molecules from the difference or similarity of the atomic temperatures in the SC and neighboring bisA molecules. It is remarkable in the M8n3 case in Fig. 8(a) that the C-temperatures are substantially lower than the O-temperatures in the SC molecules. We remind that the interatomic interaction between the SC and bisA molecules is through the van der Waals and Coulomb forces. While the van der Waals forces are similar between various atomic pairs between the SC and bisA molecules, the Coulomb forces are significant between the C and O atoms of the SC and bisA molecules, respectively, because the charges are opposite in sign and the magnitude of O charge is large (see, Fig. 1(b)). We therefore conjecture that substantial proportion of heat is transferred from the C of the SC molecule to the O of bisA molecule through the Coulomb interaction when the SC molecules are surrounded by bisA molecules as in the M8n3 case.

The conjecture mentioned above is supported by the atomic temperatures of bisA located within 5 Å of the SC atoms depicted in Fig. 10. In Fig. 10, we adopt the grouping rule of atoms used in the Dreiding inter-atomic potential: O atoms are divided into O1 (epoxy) and O2 (others); C atoms, into C2 (benzene) and C1 (others). The averaged atomic-temperatures of bisA in the M8n3 and M16n3 cases are higher than that in the M16n11 and M32n3 cases. It is much related to the increased effective interaction between the SC and bisA molecules in the M8n3 and M16n3 cases due to entanglement of the bisA to SC molecules as mentioned above. In the M16n3 case, the O1-temperature (422 K) of the bisA is higher than other temperatures (419 – 420 K) of the bisA and is close to the C-temperatures (423 – 424 K) of the SC molecule. Similarly, the O1 and O2-temperatures (420 K) of bisA are higher than other temperatures (417 – 418 K) of bisA and correspond to the average of the C and O-temperatures of the SC molecule in the M8n3 case. We therefore conclude that a substantial proportion of heat is transferred from the C of the SC molecule to the O of neighboring bisA molecules when the density of the SC molecules on the interface is not large as in the M8n3. Since the atomic temperatures are homogeneous in the M16n11 and M32n3 cases, we guess that heat is transferred from the SC to bisA

molecules through various atomic pairs when the density of the SC molecules on the interface is large or the lengths of the SC molecules are long.

V. SUMMARY AND CONCLUDING REMARKS

We have considered the simulation system composed of the bisphenol-A (bisA) epoxy region with 112 Å in z-width at the center and the α-alumina regions with (0001) surfaces to sandwich it. At the α-alumina-bisA interface, the model SC molecules have been inserted. We have constructed the inter-atomic potential between the α-alumina and the SC molecule, which is essential in the present MD simulation, based on the calculated energies with the electronic density-functional theory. We have adopted the CMAS inter-atomic potential for α-alumina and the Dreiding inter-atomic potentials for the bisA and SC molecules.

By performing the non-equilibrium MD simulation runs, we have found that the thermal resistance at the α-alumina-bisA interface becomes smaller when either larger number of the SC molecules is added at the interface or their lengths are longer. We have found that the effective thermal conductivity of the system approaches to the value estimated by assuming zero thermal resistance at the interface. On the other hand, when the number of the SC molecules is small, thermal resistance between the SC to bisA molecules is small. In the situation a substantial proportion of heat is transferred from the C of the SC molecule to the O of neighboring bisA molecules.

There exist a number of open problems that can be addressed theoretically with the MD simulation: (i) We have used the simple model molecules as the surface-coupling agent in the present simulation. Bond-formation reactions of a surface-coupling molecule with a filler material are complex combinations of hydrolysis and condensation reactions, which are ignored in the present modeling. The first-principle MD simulation[33] or hybrid quantum-classical simulation,[34,35] in which reacting atoms are treated with the DFT method, can treat such bond-formation reactions. (ii) When the packing fraction of the fillers is increased, the polymer region sandwiched by the fillers can be quite thin depending on the degree of filler agglomeration. The present simulation results cannot be applied to such a situation because we have considered the interface of bulk bisA (as polymer) and α-alumina (as filler). We are presently working on the hybrid quantum-classical simulation study of heat transfer when the bisA region is thin.

ACKNOWLEDGMENTS

This research is supported by MEXT Strategic Programs for Innovative Research (SPIRE), Computational Materials Science Initiative (CMSI), and Grant-in-Aid for Scientific Research (Kakenhi: 23310074) of Japan. The computations were performed in part using Fujitsu FX10 at Information Technology Center of the University of Tokyo, Hitachi SR16000 at Institute of Material Research of Tohoku University, Fujitsu PRIMERGY at Research Center for Computational Science (Okazaki), and Fujitsu FX10 at Institute for Solid State Physics of the University of Tokyo.

[1]S. Mallik, N. Ekere, C. Best, and R. Bhatti, Appl. Therm. Eng. **31**, 355 (2011).
[2]X. C. Tong, *Advanced Materials for Thermal Management of Electronic Packaging* (Springer, NY, 2011).
[3]R. W. Johnson, J. L. Evans, P. Jacobsen, J. R. Thompson, and M. Christopher, IEEE Trans. Electron. Packag. Manuf. **27**(3), 164 (2004).
[4]D. W. Sundstrom and Y. D. Lee, J. Appl. Polym. Sci. **16**, 3159 (1972).
[5]Z. Shi, M. Radwan, S. Kirihara, Y. Miyamoto, and Z. Jin, Appl. Phys. Lett. **95**, 224104 (2009).
[6]X. Lu and G. Xu, J. Appl. Polym. Sci. **65**, 2733 (1997).
[7]Y. Agari, A. Uneda, and S. Nagai, J. Appl. Polym. Sci. **49**, 1625 (1993).
[8]C. P. Wong and R. S. Bollampally, J. Appl. Polym. Sci. **74**, 3396 (1999).
[9]Y. S. Xu, D. D. L. Chung, and C. Mroz, Composites, Part A **32**, 1749 (2001).
[10]H. Hirano, J. Kadota, T. Yamashita, and Y. Agari, Int. J. Chem. Biol. Eng. **6**, 29 (2012).
[11]S. Pettersson and G. D. Mahan, Phys. Rev. B **42**, 7386 (1990).
[12]G. Casati, *Foundations of Physics* (Plenum, NY, 1986), Vol. 16, p. 51.
[13]S. Maruyama and S. H. Choi, Therm. Sci. Eng. **9**, 1 (2001).
[14]S. Ogata, Y. Hanai, and Y. Shibutani, J. Soc. Mater. Sci. Jpn. **55**, 754 (2006).
[15]P. K. Schelling, S. R. Phillpot, and P. Keblinski, Phys. Rev. B **65**, 144306 (2002).
[16]D. P. Sellan, E. S. Landry, J. E. Turney, A. J. H. McGaughey, and C. H. Amon, Phys. Rev. B **81**, 214305 (2010).
[17]G. Kikugawa, T. Ohara, T. Kawaguchi, E. Torigoe, Y. Hagiwara, and Y. Matsumoto, J. Chem. Phys. **130**, 074706 (2009).
[18]K. Sasikumar and P. Keblinski, J. Appl. Phys. **109**, 114307 (2011).
[19]A. R. Abramson, C.-L. Tien, and A. Majumdar, J. Heat Transfer **124**, 963 (2002).
[20]M. Hu, S. Shenogin, and P. Keblinski, Appl. Phys. Lett. **91**, 241910 (2007).
[21]T. Luo and J. R. Lloyd, Adv. Funct. Mater. **22**, 2495 (2012).
[22]M. Matsui, Phys. Chem. Miner. **23**, 345 (1996).
[23]S. L. Mayo, B. D. Olafson, and W. A. Goddard III, J. Phys. Chem. **94**, 8897 (1990).
[24]J. Gasteiger and M. Marsili, Tetrahedron **36**, 3219 (1980).
[25]B. Delley, J. Chem. Phys. **92**, 508 (1990).
[26]B. Delley, J. Chem. Phys. **113**, 7756 (2000).
[27]J. P. Perdew, K. Burke, and M. Ernzerhof, Phys. Rev. Lett. **77**, 3865 (1996).
[28]*CRC Handbook of Chemistry and Physics*, 67th ed., edited by R. C. Weast (CRC Press, Boca Raton, FL, 1983).
[29]J. B. Wachtman, Jr., W. E. Tefft, D. G. Lam, and R. P. Stinchfield, J. Res. Natl. Bur. Stand. **64A**, 213 (1960); J. B. Wachtman, Jr., in *Mechanical and Thermal Properties of Ceramics*, edited by J. B. Wachtman, Jr. (NBS, Washington, 1969), p. 139.
[30]K. C. Hass, W. F. Schneider, A. Curioni, and W. Andreoni, Science **282**(9), 265 (1998).
[31]I. Frank, D. Marx, and M. Parrinello, J. Chem. Phys. **104**, 8143 (1996).
[32]I. Manassidis, A. DeVita, and M. J. Gllian, Surf. Sci. Lett. **285**, L517 (1993).
[33]N. Ohba, S. Ogata, T. Kouno, and T. Tamura, Comput. Phys. Commun. **183**, 1664 (2012).
[34]S. Ogata, Phys. Rev. B **72**, 045348 (2005).
[35]S. Ogata, Y. Abe, N. Ohba, and R. Kobayashi, J. Appl. Phys. **108**, 064313 (2010).